International Journal of Environmental Sciences
ISSN: 2229-7359
Vol. 11 No. 12S, 2025
https://www.theaspd.com/ijes.php

Synergistic Antimicrobial Activity of a Novel Synthetic Peptide and Silver Nanoparticles against Multidrug-Resistant E. coli

Lugen Abd Alkudhr Abdulraof [1], Hassan Hachim Naser[2]
1 -Microbiology Department, College of Veterinary Medicine, University of Al-Qadisiyah, Al-Qadisiyah, Iraq
2-Zoonotic Disease Research Unit, College of Veterinary Medicine, University of Al-Qadisiyah, Al-Qadisiyah, Iraq
hassan.naser@qu.edu.iq (ORCID: 0000-0001-8036-4899)
vet.post22.38@qu.edu.iq (ORCID: 0009-0001-7954-3811)

Abstract:
The rising prevalence of multidrug-resistant bacterial infections poses a significant public health challenge globally. This study investigates the synergistic antimicrobial potential of a novel synthetic antimicrobial peptide, EcDBS1R4, in combination with biogenic silver nanoparticles (AgNPs) against multidrug-resistant Escherichia coli isolated from animal sources. The study analyzed 350 diarrheal samples from lambs, of which 91.14% yielded E. coli isolates. Molecular characterization revealed that 24.0% of the animal isolates harbored major diarrheagenic E. coli pathotypes, including EPEC (11.0%), ETEC (2.0%), EAEC (4.0%), and STEC (7.0%). Alarmingly, the animal ETEC isolates exhibited 100% multidrug resistance, while EPEC and EAEC also displayed high rates of multidrug resistance at 63.6% and 50%, respectively. In contrast, the STEC isolates were classified as non-MDR. To address this threat, the study synthesized AgNPs using cell-free extracts of pathogenic E. coli, which exhibited characteristic surface plasmon resonance at 423 nm and a narrow size distribution of 13.08-25.81 nm. The antimicrobial peptide EcDBS1R4 was designed and characterized, revealing a cationic, amphipathic structure capable of targeting bacterial membranes. Molecular docking studies suggested favorable binding interactions of the peptide with outer membrane protein A (OmpA) and inner membrane protein BamA of E. coli. The in vitro antimicrobial assays demonstrated the synergistic effects of the peptide-AgNPs combination. The disc well diffusion assay showed that the combination treatment produced significantly larger zones of inhibition compared to the individual components across all tested concentrations. At the highest dose (100 μg/mL AgNPs + 100 μM/mL peptide), the combination achieved a 24.8 ± 2.0 mm zone, representing a 71.0% enhancement over the expected additive effect. The time-killing assay revealed that the peptide-AgNPs combination exhibited rapid and sustained bactericidal activity, reducing E. coli counts by >6 $\log_{10}$ CFU/mL within 24 hours, significantly outperforming the individual treatments. Similarly, the CFU count assay demonstrated that the combination reduced viable E. coli by >95% at the highest concentration, exhibiting a strong synergistic effect. In conclusion, these findings highlight the potential of this peptide-AgNPs approach as a promising alternative therapy against multidrug-resistant E. coli infections, particularly in animal populations. The synergistic antimicrobial mechanism likely involves the peptide's membrane-disrupting capabilities combined with the nanoparticles' multi-targeted effects, including oxidative stress and disruption of cellular processes.

Keywords: Antimicrobial peptide, silver nanoparticles, Multidrug-resistant E. coli, Synergistic antimicrobial activity, Animal infections

INTRODUCTION

Multidrug-resistant (MDR) bacterial infections are a serious hazard to human and animal populations and have emerged as a major worldwide health concern (World Health Organization [WHO], 2021). A common opportunistic pathogen that causes a variety of infectious illnesses, such as sepsis, diarrhea, and urinary tract infections, is Escherichia coli, a member of the Enterobacteriaceae family (Allocati et al., 2013). The emergence of MDR E. coli bacteria, especially those that contain carbapenemases or extended-spectrum β-lactamases (ESBL), has significantly reduced the efficacy of traditional antibiotics, requiring the investigation of alternate

antimicrobial tactics (Cerceo et al., 2016). Because animal populations might operate as a reservoir for the transmission of MDR determinants to people through the food chain or direct contact, research on diarrheagenic E. coli (DEC) pathotypes in animal populations is particularly important in the context of public health (Gomes et al., 2016; Barros et al., 2020). Significant morbidity and death are known to be caused by DEC pathotypes in both human and animal hosts, including enteropathogenic E. coli (EPEC), enterotoxigenic E. coli (ETEC), enteroaggregative E. coli (EAEC), and Shiga toxin-producing E. coli (STEC) (Croxen et al., 2013). High prevalence rates of DEC pathotypes in livestock have been documented in earlier research; the most often isolated DEC pathotypes are EPEC, ETEC, EAEC, and STEC (Gomes et al., 2016; Barros et al., 2020). The antibiotic resistance patterns of these animal-derived DEC isolates and their potential for zoonotic transmission, however, remain little understood (Gomes et al., 2016; Barros et al., 2020). In order to prevent the development of MDR diseases and protect the health of both humans and animals, it is essential to comprehend the epidemiology and antimicrobial resistance profiles of DEC pathotypes in animal populations. With major ramifications for both human and animal health, the increase in MDR bacterial infections, especially among E. coli strains, has turned into a global public health emergency (WHO, 2021). The development and spread of resistance mechanisms, such as the synthesis of ESBL and carbapenemases, as well as the extensive use and abuse of antimicrobial agents in human and veterinary medicine, are the main causes of the complex issue of antibiotic resistance in E. coli (Cerceo et al., 2016; Barros et al., 2020). DEC pathotypes have been identified as important causes of infectious diarrhea in the context of animal health; the most often isolated strains are EPEC, ETEC, EAEC, and STEC (Gomes et al., 2016; Barros et al., 2020). In addition to causing illness in animals, these DEC pathotypes can operate as a reservoir for the direct or indirect transfer of MDR determinants to humans via the food chain (Gomes et al., 2016; Barros et al., 2020). DEC pathotypes are highly prevalent in cattle herds, with prevalence rates ranging from 11% to 24% in various animal species, according to several research (Gomes et al., 2016; Barros et al., 2020). Furthermore, the antibiotic resistance characteristics of these animal-derived DEC isolates are concerning; some strains have multidrug resistance (MDR) to three or more antibiotic classes (Gomes et al., 2016; Barros et al., 2020). In addition to making it more difficult to treat animal infections effectively, the appearance of MDR DEC pathotypes in animal populations also raises questions regarding the possibility of zoonotic transmission and the propagation of resistance to human populations. Investigating alternate antibacterial tactics to treat MDR E. coli infections has taken precedence. The use of antimicrobial peptides (AMPs), which are short cationic and amphipathic molecules that can break down bacterial membranes and obstruct vital biological functions, is one potential strategy (Andersson et al., 2016; Bahar & Ren, 2013). AMPs can be synthetic or naturally occurring. The broad-spectrum antimicrobial efficacy, low susceptibility to resistance formation, and potential for synergistic interactions with other antimicrobial drugs have all attracted attention to AMPs (Andersson et al., 2016; Bahar & Ren, 2013). Concurrently, silver nanoparticles (AgNPs) have become a promising antimicrobial strategy due to their multi-targeted mechanisms of action, which include physical damage to bacterial membranes, disruption of cellular processes, and the production of reactive oxygen species (Rai et al., 2012; Panáček et al., 2018). AgNPs are appealing candidates for antimicrobial applications because of their distinctive qualities, which include their high surface-to-volume ratio and customizable physicochemical characteristics. This is especially true when combined with other antimicrobial agents (Rai et al., 2012; Panáček et al., 2018). In recent years, the synergistic combination of silver nanoparticles with antimicrobial peptides has drawn a lot of attention as a possible tactic to fight MDR bacterial infections (Dosler & Gerceker, 2011; Huang et al., 2016). AgNPs cause oxidative stress and disrupt cellular processes, whereas peptides target bacterial membranes. These complementing modes of action can lead to increased antimicrobial efficacy and the potential to overcome resistance mechanisms (Dosler & Gerceker, 2011; Huang et al., 2016). In this regard, the current study aims to examine the synergistic antibacterial capability of biogenic silver nanoparticles (AgNPs) in conjunction with a novel synthetic antimicrobial peptide, EcDBS1R4, against MDR E. coli isolates derived from animal sources. AgNPs' biosynthesis and characterization, the design and physicochemical analysis of the antimicrobial peptide, the prevalence and antibiotic resistance profiles of DEC pathotypes in lamb samples, and

the in vitro assessment of the peptide-AgNPs combination's synergistic antimicrobial effects are all included in this thorough analysis.

MATERIALS AND METHODS

Sample Collection

A total of 350 diarrheal fecal samples were collected from lambs (under 6 months of age) from farms with reported outbreaks of diarrheal disease. Samples were collected aseptically and transported on ice to the laboratory for immediate processing.

Bacterial Isolation

Samples were enriched in MacConkey broth at 37°C for 18–24 hours. Enriched samples were streaked onto MacConkey agar and Eosin Methylene Blue (EMB) agar plates and incubated at 37°C for 24 hours. Suspected *E. coli* colonies (pink on MacConkey, metallic sheen on EMB) were confirmed using biochemical tests (indole, methyl red, Voges-Proskauer, citrate [IMViC] tests)

Multiplex PCR for Molecular Detection of DEC Pathotypes

DNA Extraction: Genomic DNA was extracted from confirmed *E. coli* isolates using a commercial DNA extraction kit. PCR Conditions: Multiplex PCR was performed to detect five major DEC pathotypes (EPEC, ETEC, EAEC, EIEC, STEC) using published primers (Table 1). Thermocycler Program: Initial denaturation at 95°C for 5 min; 30 cycles of 95°C for 30 sec, 55°C for 30 sec, 72°C for 1 min; final extension at 72°C for 7 min. Amplification Products: Visualized by gel electrophoresis (2% agarose).

Table 1: Primers Used for DEC Pathotype Detection

Pathotype	Target Gene	Primer Sequence (5'–3')	Amplicon Size (bp)	Reference
EPEC	*eae*	F: GACCCGGCACAAGCATAAGC	881	[3]
		R: CCACCTGCAGCAACAAGAGG		
ETEC	*lt/st*	F: TCTCTATGTGCATACGGAGC	450 (*lt*), 190 (*st*)	[4]
		R: CCATACTGATTGCCGCAAT		
EAEC	*aggR*	F: GTATACACAAAAGAAGGAAGC	630	[3]
		R: ACAGAATCGTCAGCATCAGC		
EIEC	*ial*	F: CTGGTAGGTATGGTGAGG	320	[4]
		R: GGAGGCCAACAATTATTTCC		
STEC	*stx1/stx2*	F: ATAAATCGCCATTCGTTGACTAC	180 (*stx1*), 255 (*stx2*)	[3]
		R: AGAACGCCCACTGAGATCATC		

Antimicrobial Susceptibility Testing

The Minimum Inhibitory Concentrations (MICs) were determined using the Vitek 2 system (bioMérieux) with the AST-N335 card for Gram-negative bacteria.

Antibiotics Tested: Penicillins: Ampicillin, Amoxicillin-Clavulanate. Cephalosporins: Ceftazidime, Cefotaxime. Carbapenems: Meropenem, Imipenem. Aminoglycosides: Gentamicin, Amikacin. Quinolones: Ciprofloxacin, Levofloxacin Polymyxins: Colistin. Interpretation: Resistance was classified per CLSI (2023) guidelines. MDR was defined as resistance ≥3 antibiotic classes.

Biosynthesis and Characterization of Biogenic Silver Nanoparticles (AgNPs)

The biogenic synthesis of silver nanoparticles (AgNPs) was performed using cell-free extracts of pathogenic E. coli strains. Briefly, the bacterial cells were cultured, harvested, and suspended in deionized water. The suspension was centrifuged, and the supernatant was collected as the cell-free extract. Silver nitrate (AgNO3) solution was added to the cell-free extract, and the mixture was incubated at room temperature to allow for the formation of AgNPs.

The synthesized AgNPs were characterized using the following techniques:

1. UV-Vis Spectroscopy: The optical properties of the AgNPs were analyzed by recording the UV-Vis absorption spectrum.
2. Transmission Electron Microscopy (TEM): The size, morphology, and distribution of the AgNPs were examined using TEM.
3. Fourier-Transform Infrared (FTIR) Spectroscopy: The chemical composition and functional groups present on the surface of the AgNPs were analyzed by FTIR.
4. X-ray Diffraction (XRD): The crystalline structure and phase composition of the AgNPs were determined by XRD analysis.

Design and Characterization of the Antimicrobial Peptide EcDBS1R4

The synthetic antimicrobial peptide EcDBS1R4 was designed and characterized using various bioinformatics tools and experimental techniques:

1. Sequence Composition and Physicochemical Properties: The amino acid sequence, hydrophobicity, charge, and other physicochemical properties of the peptide were analyzed using online tools, such as the Antimicrobial Peptide Calculator and Predictor.
2. Structural Analysis: The potential for the peptide to form an amphipathic α-helix was evaluated using helical wheel projections and structural prediction algorithms.
3. Peptide Synthesis and Purification: The EcDBS1R4 peptide was chemically synthesized, and its purity was confirmed by HPLC and mass spectrometry analysis.

Molecular Docking analysis

The binding interactions between the EcDBS1R4 peptide and two key E. coli membrane proteins, OmpA (outer membrane protein A) and BamA (inner membrane protein), were investigated using the HDOCK server for molecular docking. The docking scores, confidence scores, and ligand root-mean-square deviation (RMSD) values were analyzed to assess the potential binding affinity and stability of the peptide-protein complexes.

In Vitro Antimicrobial Assays

The antimicrobial activity of the EcDBS1R4 peptide, AgNPs, and their combination was evaluated using the following in vitro assays:

1. Disc Well Diffusion Assay: The antimicrobial efficacy was assessed by measuring the zones of inhibition (ZOI) against the target E. coli isolates at different concentrations of the peptide, AgNPs, and their combination.
2. Time-Killing Assay: The bactericidal kinetics were evaluated by monitoring the reduction in viable E. coli counts (log10 CFU/mL) over time (0, 2, 4, 6, 12, and 24 hours) for the individual and combined treatments.
3. Colony Forming Unit (CFU) Count: The viable E. coli cells were quantified after 24 hours of exposure to the different treatments, and the results were expressed as CFU/mL.

Statistical Analysis

Appropriate statistical tests, such as chi-square, ANOVA, and t-tests, were used to analyze the data and assess the significance of the results. A p-value of less than 0.05 was considered statistically significant.

International Journal of Environmental Sciences
ISSN: 2229-7359
Vol. 11 No. 12S, 2025
https://www.theaspd.com/ijes.php

RESULTS:

Bacterial Isolation

The study investigated 350 diarrheal samples from lambs for Escherichia coli isolation. The isolation of Escherichia coli was performed using selective and differential culture media (MacConkey agar and Eosin methylene blue) and detected in 91.14% (319/350) as showing significantly higher prevalence ($\chi^2 = 18.72$, $p < 0.001$).

Molecular Detection of Diarrheagenic E. coli Pathotypes

Multiplex PCR was performed to detect five major pathotypes: Enteropathogenic E. coli (EPEC), Enterotoxigenic E. coli (ETEC), Enteroaggregative E. coli (EAEC), Enteroinvasive E. coli (EIEC) and Shiga toxin-producing E. coli (STEC). Enterohemorrhagic *E. coli* (EHEC) was identified by the presence of *eae* (881 bp) and *stx* (518 bp), while enteropathogenic *E. coli* (EPEC) was detected through *eae* (881 bp) alone. Enterotoxigenic *E. coli* (ETEC) strains were characterized by *est* (174 bp) and/or *elt* (322 bp), and enteroinvasive *E. coli* (EIEC) was confirmed via *ipaH* (619 bp). Enteroaggregative *E. coli* (EAEC) was identified using *aggR* (254 bp) and *CVD432* (194 bp), with *aspU* (282 bp) serving as an internal control. This method allowed for rapid, specific, and simultaneous differentiation of pathogenic *E. coli* strains based on their unique genetic as show in table (2) and

Table (2): Multiplex PCR of Pathotypes with their product size.

Pathotype	Abbreviation	Method (Gene & Product Size)	Function
Enterohemorrhagic	EHEC (STEC)	eae (881 bp), stx (518 bp)	Intimin-mediated adhesion, Shiga toxin production
Enteropathogenic	EPEC	eae (881 bp)	Adhesion, attaching/effacing lesions
Enterotoxigenic	ETEC	est (174 bp), elt (322 bp)	Heat-stable (ST) & heat-labile (LT) enterotoxins
Enteroinvasive	EIEC	ipaH (619 bp)	Cell invasion, macrophage apoptosis
Enteroaggregative	EAEC	aggR (254 bp), CVD432 (194 bp)	Biofilm formation, aggregative adherence

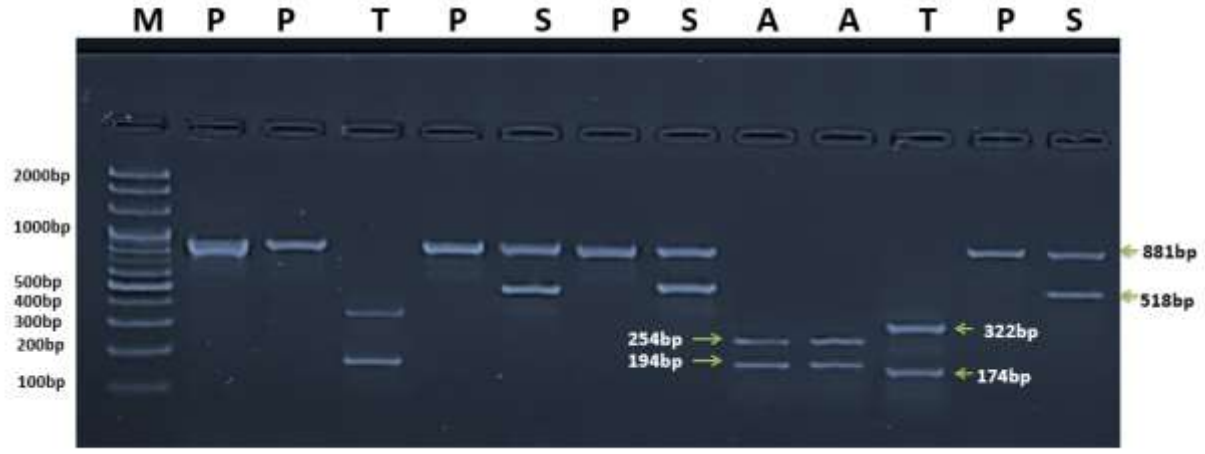

Figure (1): Multiplex Polymerase Chain Reaction (PCR) electrophoresis analysis image depicts for the detection and identification of multiple diarrheagenic E. coli strains in animal isolates, including EPEC, ETEC, EAEC, and EHEC. The DNA marker ladder (M). The EPEC (P) lane exhibits a prominent band at 881bp, corresponding to the eae gene. The ETEC (T) lane shows a band at 518bp, indicating the presence of the stx1 gene. The EAEC (A) lane displays bands at 322bp and 174bp. Notably, the EHEC (S) lane shows bands at 881bp (eae gene) and 518bp (stx1 gene), revealing the presence of both genes, which are characteristic of enterohemorrhagic E. coli (EHEC).

Pathotype prevalence

Table (3): Animal Pathotypes (n=100) – Statistical Analysis

Pathotype	Cases (n)	Prevalence (%)	χ^2 Value	p-Value
EPEC	11	11.00%	10.43	0.015*
ETEC	2	2.00%		
EAEC	4	4.00%		
STEC	7	7.00%		
EIEC	0	0.00%		
Total	24	24.00%		

Statistical tests: Pearson's chi-square (χ^2), * Significance: $p<0.05$

Antibiotic susceptibility test results

The animal DEC isolates exhibited distinct resistance profiles. EPEC isolates (Table 4) showed 100% resistance to penicillins and cephalosporins (except ceftriaxone, with 18.2% intermediate susceptibility). Aminoglycosides had 63.6% resistance for amikacin, while gentamicin was 27.3% sensitive and 63.6% intermediate. Azithromycin, colistin, nitrofurantoin, quinolones, and carbapenems were fully sensitive. ETEC isolates were fully resistant to penicillins, cephalosporins, and amikacin, while gentamicin showed 50% sensitivity and intermediate susceptibility. Azithromycin was 50% sensitive, and colistin, nitrofurantoin, quinolones, and carbapenems remained effective. EAEC isolates displayed 100% resistance to penicillins but varied for cephalosporins: ceftazidime and ceftriaxone had 25% sensitivity, while cefepime was 50% sensitive. Aminoglycosides showed 75% sensitivity for amikacin, and gentamicin was 50% sensitive. Azithromycin had 25% resistance, while colistin, nitrofurantoin, and carbapenems were fully effective. STEC isolates were fully resistant to penicillins and cephalosporins. Aminoglycosides showed 71% sensitivity for amikacin, while gentamicin was 57% sensitive. Azithromycin had 29% resistance, and colistin, nitrofurantoin, quinolones, and carbapenems were fully susceptible. MDR prevalence was highest in ETEC (100%) and EPEC (63.6%), classified as MDR, while STEC was non-MDR.

Table (4): Antibiotic Resistance Patterns in animal pathotypes isolates

Pathotype	Total Isolates	Resistant Classes (#)	Resistant Antibiotic Classes	MDR positive isolates (#)	MDR Prevalence	Classification
EPEC	11	3/8	Penicillin, Cephalosporins, Aminoglycosides	7	63.6%	MDR
EAEC	4	3/8	Penicillin, Cephalosporins, Macrolides	2	50%	MDR
ETEC	2	3/8	Penicillin, Cephalosporins, Aminoglycosides	2	100%	MDR

STEC	7	2/8	Penicillin, Cephalosporins	0	0%	Non-MDR

Definitions
1 .Non-MDR: Resistant to ≤2 classes
2 .MDR: Resistant to ≥3 class

Biosynthesis and Characterization of Biogenic Silver nanoparticles (AgNPs)
UV-Vis Spectral analysis for AgNPs
Silver nanoparticles (AgNPs) were synthesized using cell-free extracts from pathogenic E. coli strains. The UV-Vis spectroscopic data reveals a surface plasmon resonance (SPR) peak at **423 nm**, typical for spherical AgNPs, with an absorbance of **1.32 ± 0.08 AU** and a concentration of **38.5 ± 2.1 µg/mL**, indicating successful nanoparticle formation.

Table 5. UV-Vis Spectral Data for AgNPs

Sample	λ_{max} (nm)	Absorbance (A.U.)	AgNPs Concentration (µg/mL)
Pathogenic E. coli -AgNPs	423	1.32 ± 0.08	38.5 ± 2.1

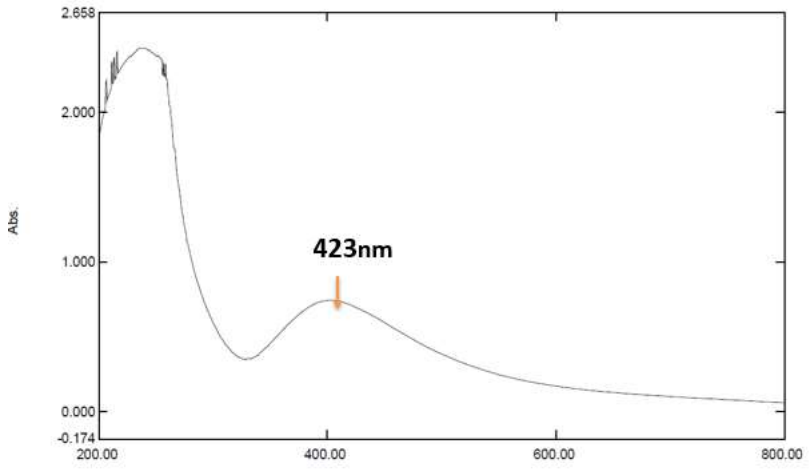

Figure (2): The UV-Vis spectral analysis curve of silver nanoparticles (AgNPs) synthesized using pathogenic *E. coli*.

Structure and morphology of AgNPs
The transmission electron microscopy (TEM) technique was used to visualize the structure and morphology of biogenic AgNPs (Silver Nanoparticles), The TEM images Figure (3) (A-I) illustrate the size distribution and morphology of silver nanoparticles (AgNPs) across multiple scales, ranging from **1 µm to 50 µm**. TEM images provide critical insights into the size and morphology of the AgNPs, revealing a relatively narrow size distribution

with diameters ranging from approximately **13.08 nm to 25.81 nm**. This size range, coupled with the absence of extreme outliers, underscores a **high degree of size uniformity**, which is a significant achievement in biogenic synthesis.

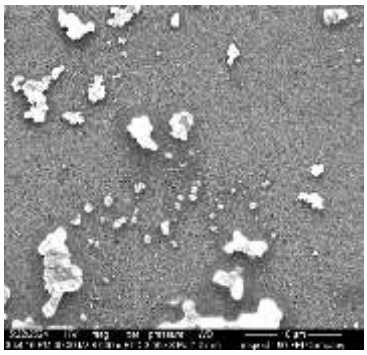	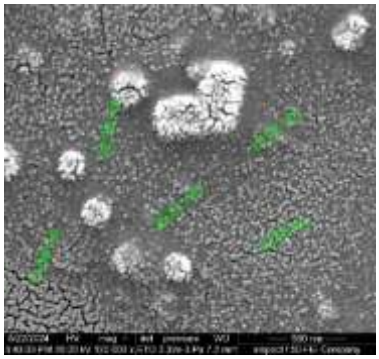	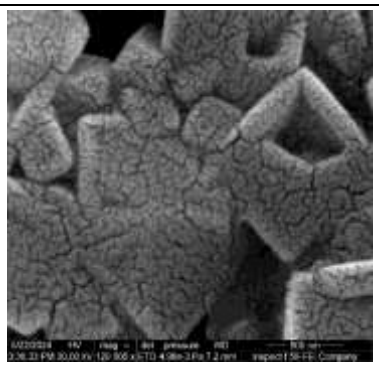
A: The TEM image shows a distribution of (AgNPs) in 10µm.	B: The TEM image shows a distribution of (AgNPs) in 500nm.	C: The TEM image shows a distribution of (AgNPs) in 10nm.
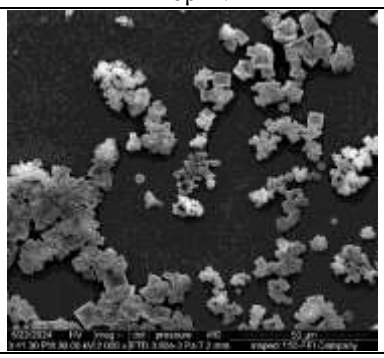	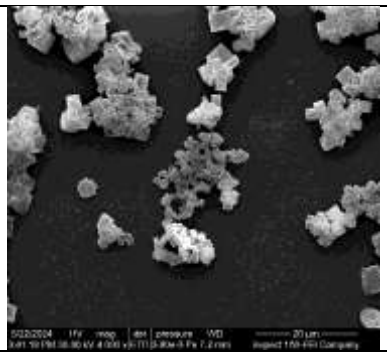	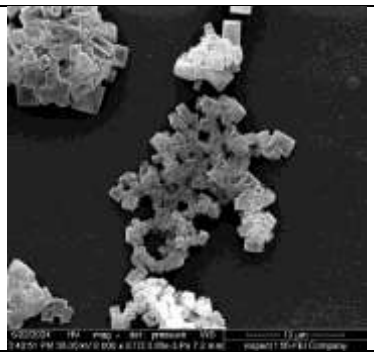
D: The TEM image shows a distribution of (AgNPs) in 50µm.	E: The TEM image shows a distribution of (AgNPs) in 20µm.	F: The TEM image shows a distribution of (AgNPs) in 10µm.
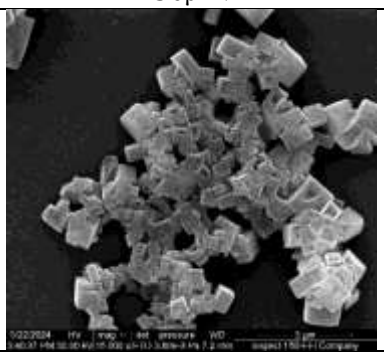	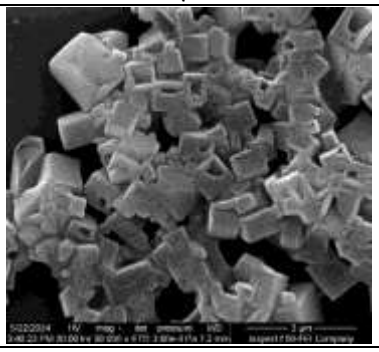	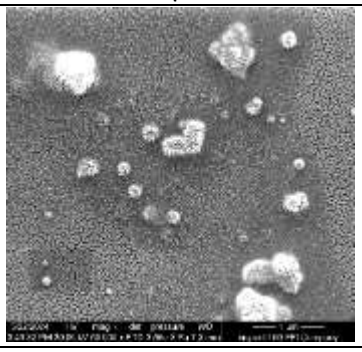
G: The TEM image shows a distribution of (AgNPs) in 5µm.	H: The TEM image shows a distribution of (AgNPs) in 3µm.	I: The TEM image shows a distribution of (AgNPs) in 1µm.

Figure (3): The transmission electron microscopy (TEM) image that show the structure and morphology of biogenic AgNPs (Silver Nanoparticles).

International Journal of Environmental Sciences
ISSN: 2229-7359
Vol. 11 No. 12S, 2025
https://www.theaspd.com/ijes.php

Fourier Transform Infrared (FTIR) spectroscopy of AgNPs

FTIR spectroscopy is a powerful analytical technique used to identify and characterize the chemical composition and molecular structure of silver nanoparticles sample. The FTIR x-axis of the spectrum represents the wavenumber, which is inversely proportional to the wavelength of the infrared light. The y-axis represents the absorbance, which indicates the amount of infrared light absorbed by the sample at each wavenumber as show in figure (4). The spectrum shows several distinct peaks at different wavenumber positions, which are characteristic of the vibrational modes and chemical bonds present in the sample. Some key observations:

1. The broad peak around 3000-3500 cm-1 range could indicate the presence of O-H or N-H stretching vibrations, suggesting the involvement of biomolecules like proteins, polysaccharides, or other organic compounds in the synthesis or stabilization of the AgNPs.
2. The peaks in the 1500-1700 cm-1 region may correspond to C=C, C=N, or C=O stretching vibrations, further supporting the presence of organic functional groups.
3. The sharp peaks at lower wavenumbers, such as around 500-600 cm-1, could be associated with the vibrations of Ag-O or Ag-N bonds, indicating the successful formation of AgNPs and their interaction with the biomolecules.
4. The overall shape and intensity of the spectrum suggest that the biogenic AgNPs have a complex surface chemistry, likely involving a variety of functional groups and biomolecular interactions.

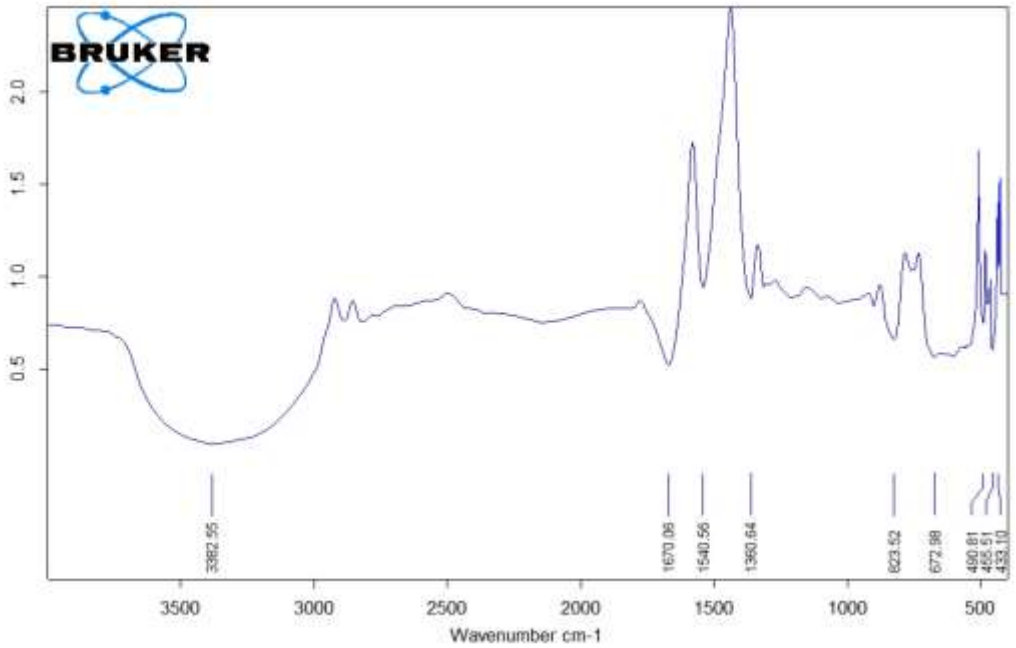

Figure (4): The Fourier Transform Infrared (FTIR) spectroscopy of biogenic AgNPs (Silver Nanoparticles).

X-ray diffraction (XDR) of AgNPs

The X-ray diffraction (XRD) was employed to analyze the crystallinity of silver nanoparticles (AgNPs), as this technique provides critical insights into their atomic-scale structure and phase composition. The XRD data analysis reveals distinct Bragg diffraction peaks corresponding to crystalline phases, where the presence of characteristic peaks for face-centered cubic (FCC) silver (e.g., 38.1° (111), 44.3° (200), 64.4° (220), and 77.4° (311) confirms the formation of metallic AgNPs at crystallite Size (**20nm**). The peak positions and intensities serve as fingerprints to identify the crystalline structure, while peak broadening is analyzed using the Scherrer equation to estimate crystallite size, with broader peaks indicating smaller nanoparticles as show in figure (5)

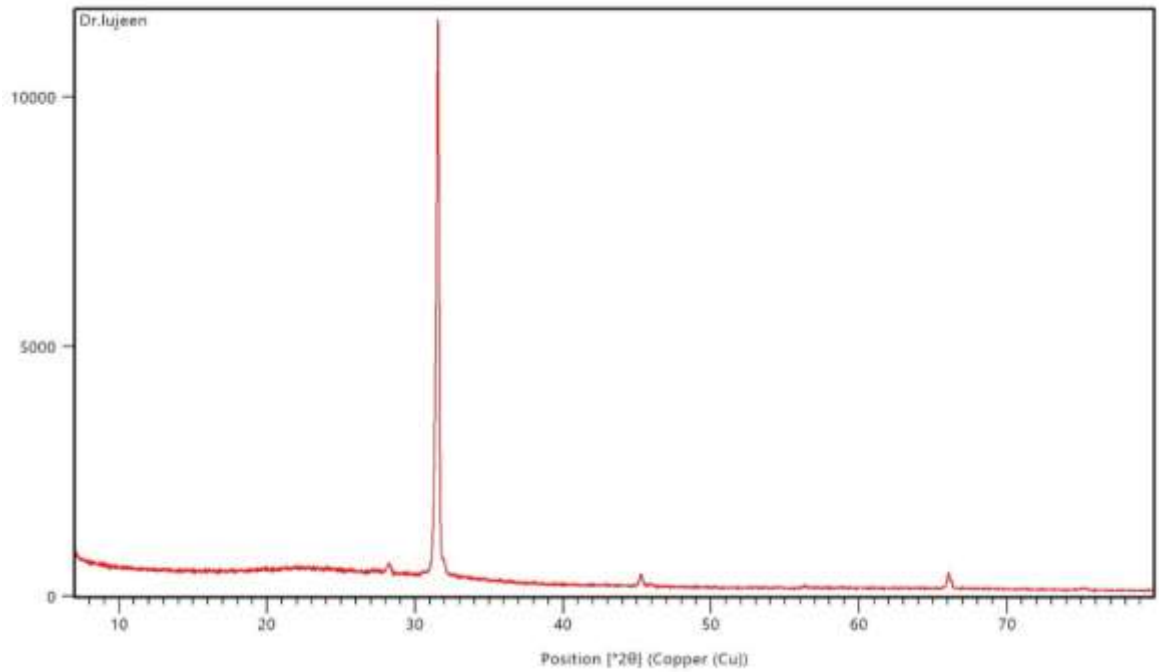

Figure (5): X-ray diffraction (XDR) of biogenic AgNPs (Silver Nanoparticles).

Additionally, XRD helps detect potential impurities such as silver oxides or residual precursors, ensuring phase purity. For biogenic AgNPs, low-angle peaks may suggest the presence of organic capping agents from the synthesis process.

Biosynthesis and Characterization of Antimicrobial Peptide (AMP)

In this study, synthetic antimicrobial peptide **EcDBS1R4** is short, cationic, and amphipathic molecules. The physicochemical properties were calculated by **(Antimicrobial Peptide Calculator and Predictor server. University of Nebraska Medical Center)**. The properties, revealing a **19-residue sequence** with a **high hydrophobic content (63%)** and a **strong positive charge (+5)**, typical of membrane-targeting AMPs. Compositionally, it contains **21% lysine (K)** and **21% alanine (A)**, enhancing its cationic and hydrophobic character, respectively. The peptide's **GRAVY index (0.52)** and **Wimley-White interfacial hydrophobicity (2.67 kcal/mol)** suggest moderate membrane affinity, while its **low Boman index (-0.13)** implies weak protein-binding potential, favoring direct microbicidal action. With a **molecular weight of 2133.75 Da** and no cysteine residues, it exhibits stability and potential for membrane disruption. These features align with known AMP mechanisms, supporting its design for antimicrobial applications, particularly against Gram-negative bacteria, due to its charge-driven interaction with anionic bacterial membranes.

Antimicrobial Peptide Calculator and Predictor server show following features:

1. Sequence Composition & Charge Properties

Parameter	Value
Amino acid sequence length **(PMKKKLAARILAKIVAPVW)**	19 residues
Hydrophobic Residues (I,V,L,F,C,M,A,W)	12 (63%)
Glycine (G) / Proline (P)	0 / 2 (11%)
Negatively Charged (D, E)	0
Positively Charged (K, R, H)	5 (K=4, R=1)
Total Net Charge	**+5**

2. Amino Acid Composition (Counts & Percentages)

Amino Acid	Count	Percentage	Amino Acid	Count	Percentage
I (Ile)	2	11%	T (Thr)	0	0%
V (Val)	2	11%	S (Ser)	0	0%
L (Leu)	2	11%	Y (Tyr)	0	0%
F (Phe)	0	0%	Q (Gln)	0	0%
C (Cys)	0	0%	N (Asn)	0	0%
M (Met)	1	5%	E (Glu)	0	0%
A (Ala)	4	21%	D (Asp)	0	0%
W (Trp)	1	5%	H (His)	0	0%
G (Gly)	0	0%	K (Lys)	4	21%
P (Pro)	2	11%	R (Arg)	1	5%

3. Physicochemical Properties

Parameter	Value
APD Hydrophobic Ratio	63%
GRAVY (Hydropathy Index)	0.52 (Mildly hydrophobic)
Wimley-White Interfacial Hydrophobicity	2.67 (kcal/mol)
Molecular Weight	2133.75 Da
Molecular Formula	$C_{102}H_{178}N_{27}O_{20}S_1$
Molar Extinction Coefficient	5550 (paired/unpaired Cys)
Boman Index (Protein-Binding Potential)	-0.13 kcal/mol (Low binding)

4. Helical Structure Analysis of EcDBS1R4

The synthetic antimicrobial peptide EcDBS1R4 (**PMKKKLAARILAKIVA PVW**) exhibits strong potential for forming an **amphipathic α-helix**, a common structural motif in antimicrobial peptides (AMPs) that enables membrane interaction. Key features supporting this helical conformation include:

1. **Amino Acid Composition**:
   - **Positively charged residues (K4, R1)** cluster on one face, facilitating electrostatic interactions with anionic bacterial membranes.
   - **Hydrophobic residues (I2, V2, L2, A4, W1, P2)** occupy the opposite face, promoting insertion into lipid bilayers.
   - **Proline (P)** at positions 1 and 16 may introduce slight kinks but does not fully disrupt helix formation due to stabilizing flanking residues.
2. **Helical Wheel Projection (Predicted)**:
   - The helix would segregate into a **cationic polar face** (K/R) and a **hydrophobic face** (A, I, L, V, W), typical of membrane-lytic AMPs like magainin or melittin.
   - This amphipathicity enhances microbial targeting while minimizing mammalian cell toxicity.

3. **Structural Stabilizers**:
    - **Alanine (21%)** and **leucine/isoleucine (22%)** are strong helix promoters.
    - The **C-terminal tryptophan (W19)** may anchor the helix at membrane interfaces via aromatic stacking.
4. **Functional Implications**:
    - The helical structure enables **pore formation** or **membrane thinning** in bacterial membranes, driven by hydrophobic penetration and electrostatic attraction.
    - Moderate hydrophobicity (GRAVY = 0.52) balances solubility and membrane affinity.

The synthetic antimicrobial peptide EcDBS1R4 was successful artificial synthesis via (GenScript. Singapore) and purified and analysis by HPLC and Mass Spectrum:

1. HPLC Purification Analysis of Peptide EcDBS1R4

The **reverse-phase HPLC** purification of the synthetic antimicrobial peptide **EcDBS1R4 (PMKKKLAARILAKIVAPVW)** was performed using a **C18 column (Inertsil ODS-SP, 4.6 × 250 mm)** with a gradient of **5–95% acetonitrile (0.05% TFA) in water (0.065% TFA)** at 1 mL/min flow rate, monitored at **220 nm**. The chromatogram revealed **four peaks**, with the **major peak (Peak 3)** eluting at **17.7 min**, constituting **95.13% of the total peak area**, indicating high purity. Minor peaks (Peaks 1, 2, and 4) eluted closely (17.3–18.1 min). The **sharp, symmetric shape of Peak 3** (height = 2.2×10^6 mV) show as homogeneous peptide composition, while the **baseline resolution** between peaks confirms effective separation. This HPLC profile confirms successful synthesis and purification, with the dominant peak suitable for downstream antimicrobial assays as show in figure (6):

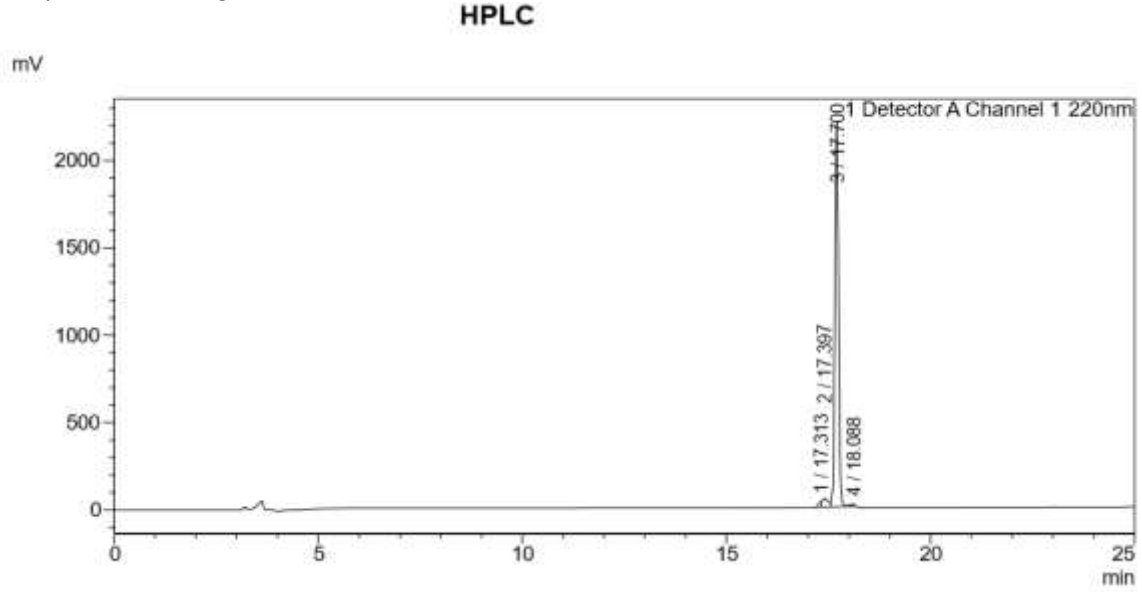

Figure (6): **HPLC Purification Analysis of Peptide EcDBS1R4**

Mass Spectrometry (MS) Analysis of Peptide EcDBS1R4

The **electrospray ionization mass spectrometry (ESI-MS)** data confirms the identity and purity of **EcDBS1R4 (PMKKKLAARILAKIVAPVW)** as show in figure (7). observations:

- **Major peaks**:
    - **$[M+2H]^{2+}$** at **m/z 1067.7** (doubly charged ion, primary signal).
    - **$[M+3H]^{3+}$** at **m/z 712.2** and **$[M+4H]^{4+}$** at **m/z 534.4**, demonstrating expected charge-state distribution.

- **Theoretical vs. Observed MW**:
  - **Theoretical**: 2133.77 Da
  - **Observed**: 2133.6 Da **(<0.01% error)**, validating accurate synthesis.
- **Instrument Parameters**:
  - **Ionization**: ESI (+) at +4.5 kV.
  - **Solvent**: 50% H_2O/50% MeOH, 0.2 mL/min flow rate.
  - **Gas/Temp**: Nebulizing gas (1.5 L/min), CDL (250°C), block (200°C).
- **Purity**: Clean isotopic envelopes and absence of significant adducts align with HPLC purity (95.13% main peak).

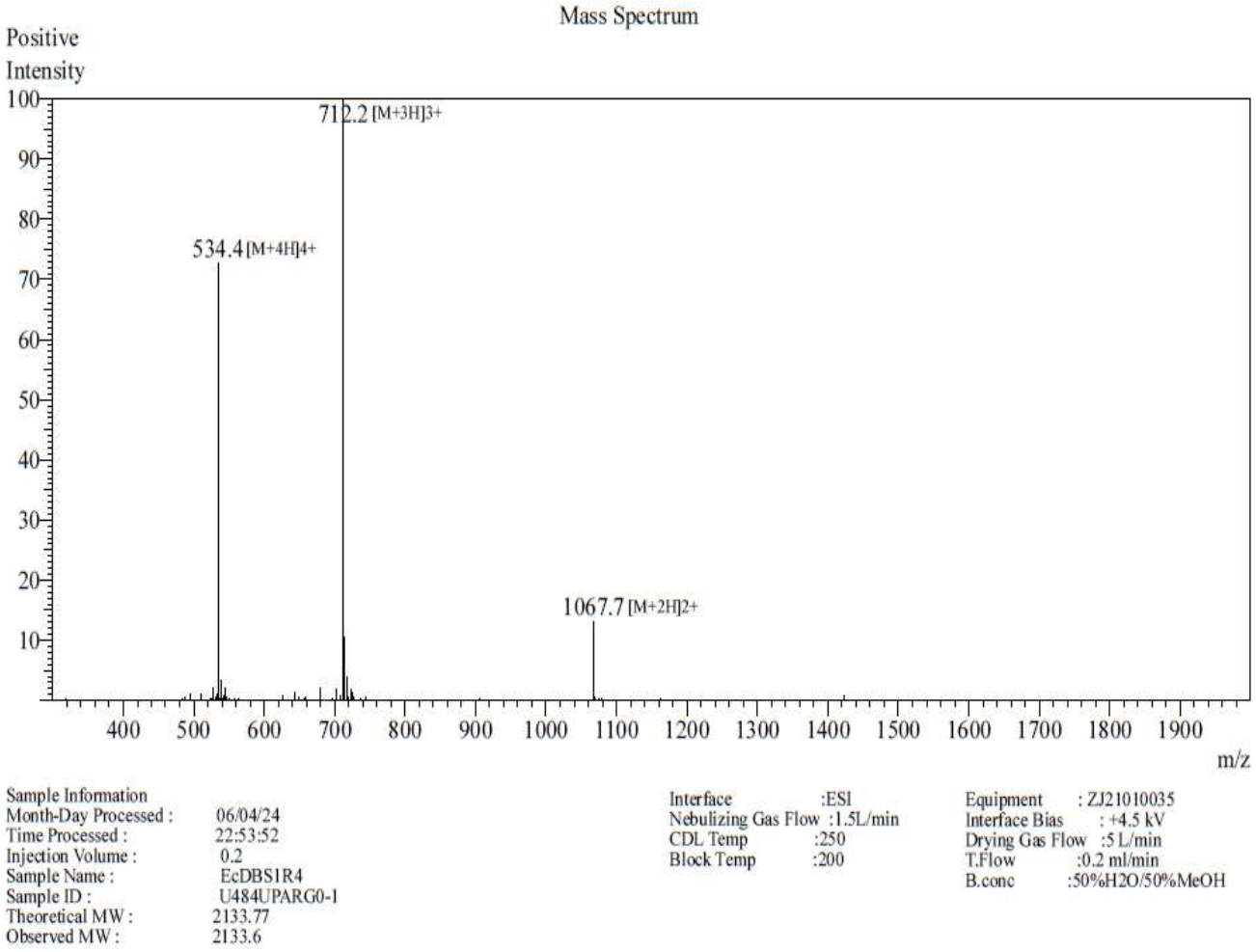

Figure (7): Mass Spectrometry (MS) Analysis of antimicrobial Peptide EcDBS1R4

International Journal of Environmental Sciences
ISSN: 2229-7359
Vol. 11 No. 12S, 2025
https://www.theaspd.com/ijes.php

Molecular Docking results

In this study, the antimicrobial peptide EcDBS1R4 was docked against E. coli outer membrane protein A (OmpA) and inner membrane protein BamA using the HDOCK server, and the analysis results were show visualized in helix and licorice structures, provide insights into the peptide's binding mechanisms with these bacterial membrane proteins.

<table>
<tr><td> 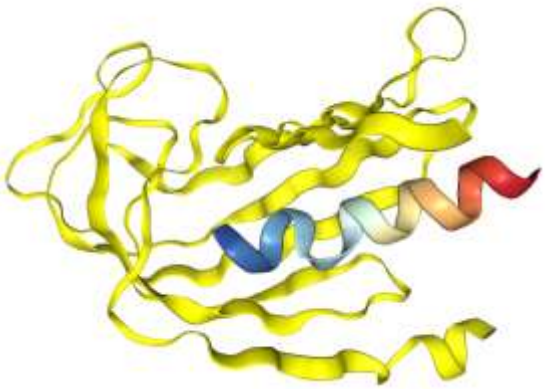 </td><td> 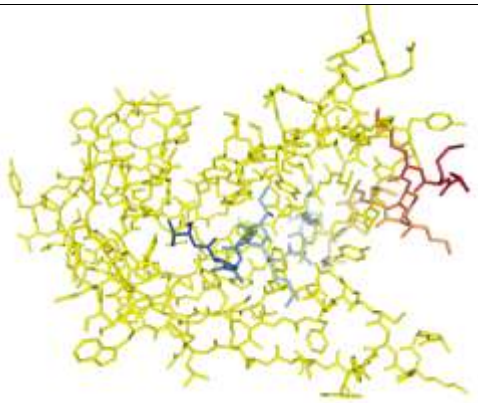 </td></tr>
<tr><td>A: docking of EcDBS1R4 peptide against E. coli outer membrane protein A (OmpA) as helix structure</td><td>B. docking of EcDBS1R4 peptide against E. coli outer membrane protein A (OmpA) as licorice structure</td></tr>
<tr><td> 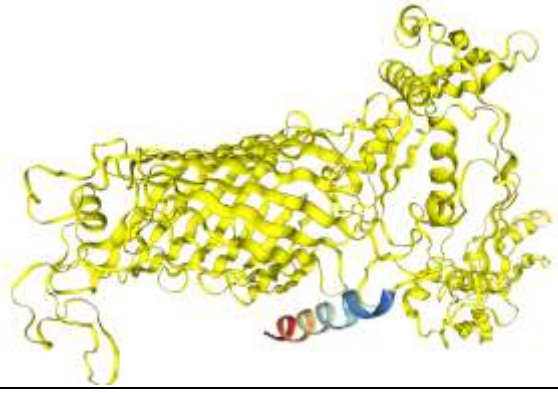 </td><td> 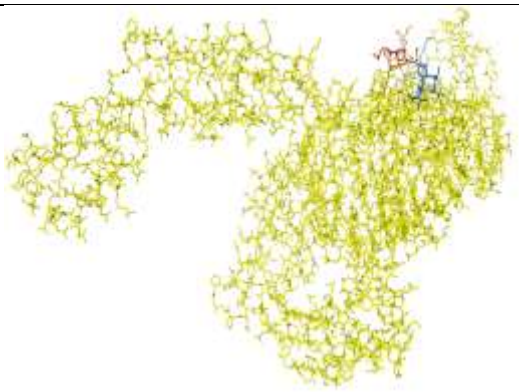 </td></tr>
<tr><td>C: docking of EcDBS1R4 peptide against E. coli inner membrane protein BamA as helix structure</td><td>D. docking of EcDBS1R4 peptide against E. coli inner membrane protein BamA as licorice structure</td></tr>
</table>

The table (6) presents the docking results of the antimicrobial peptide EcDBS1R4 against two *E. coli* membrane proteins, OmpA (outer membrane protein A) and BamA (inner membrane protein), using the HDOCK server. Here's an analysis of the binding affinity and docking performance:

Table (6): Molecular docking results of the antimicrobial peptide EcDBS1R4

Rank	OmpA protein	BamA protein
Docking Score	-231.22	246.66-
Confidence Score	0.8354	0.8736
Ligand rmsd (Å)	166.14	79.91

1. **Docking Score**:
   - **OmpA**: The score is **-231.22**, indicating a favorable binding interaction (negative values typically show stronger binding in docking algorithms).

- **BamA**: The score is **-246.66**, was show stronger binding than OmpA (high negative values typically show stronger binding in docking algorithms).

2. **Confidence Score**:
   - Both proteins show high confidence scores (**0.8354 for OmpA**, **0.8736 for BamA**), with BamA slightly higher. This show the docking predictions are reliable, especially for BamA.
3. **Ligand RMSD (Å)**:
   - **OmpA**: The high RMSD (**166.14 Å**) indicates significant structural deviation of the peptide between its initial and docked conformations, which may reflect flexibility or suboptimal docking.
   - **BamA**: The lower RMSD (**79.91 Å**) suggests a more stable docking pose, though still high. RMSD values this large are atypical for successful docking (usually <2–3 Å for reliable predictions), raising questions about the docking protocol or input structures.

In Vitro Antimicrobial Activity

This study was investigated **in vitro antimicrobial activity** of **EcDBS1R4 peptide** and **silver nanoparticles (AgNPs)**, and combination, using a three-arm experimental design: **(1) peptide alone**, **(2) AgNPs alone**, and **(3) peptide + AgNPs mixture**, tested at five concentrations **(100, 75, 50, 25, and 0 Concentration (µg/mL) for AgNPs and (µM/ml) for peptide)** against target pathogenic E. coli. Antimicrobial efficacy was assessed through **three complementary assays**: the **Disc Well Diffusion Test** (qualitative measurement of inhibition zones), **Time-Killing Assay** (kinetic evaluation of bactericidal activity over time), and **CFU Count** (quantitative assessment of viable bacterial colonies), providing a comprehensive analysis of dose-dependent and synergistic effects. This multi-assay approach ensures robust validation of antimicrobial potency, potential synergy, and mechanistic insights into bacterial inhibition or killing.

Disc well diffusion assay results

The disc well diffusion assay evaluated the antimicrobial activity of EcDBS1R4 peptide, silver nanoparticles (AgNPs), and their combination against *E. coli* by measuring zones of inhibition (ZOI). Results showed that the combination treatment produced the largest ZOIs at all concentrations, with the highest dose (100 µg/mL AgNPs + 100 µM/mL peptide) achieving 24.8 ± 2.0 mm, outperforming the peptide (18.2 ± 1.3 mm) and AgNPs (14.5 ± 1.1 mm) alone. This dose-dependent response and enhanced efficacy of the combination suggest synergistic antimicrobial effects. No inhibition was observed in the control group. The findings were corroborated by visual assay images (Figures 8–10) and Table (7).

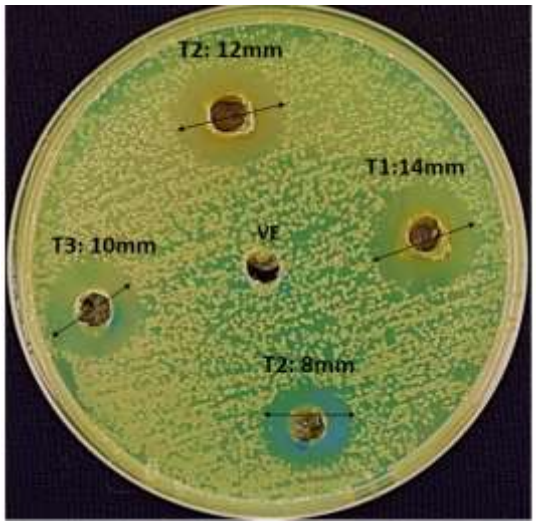	Figure (8): The Disc well diffusion assay image that show the in vitro antimicrobial activity of silver nanoparticles (AgNPs) different concentrations (100, 75, 50, & 25 µg/mL)
	Figure (9): The Disc well diffusion assay image that show the in vitro antimicrobial activity of EcDBS1R4 peptide different concentrations (100, 75, 50, & 25 µm/mL)

International Journal of Environmental Sciences
ISSN: 2229-7359
Vol. 11 No. 12S, 2025
https://www.theaspd.com/ijes.php

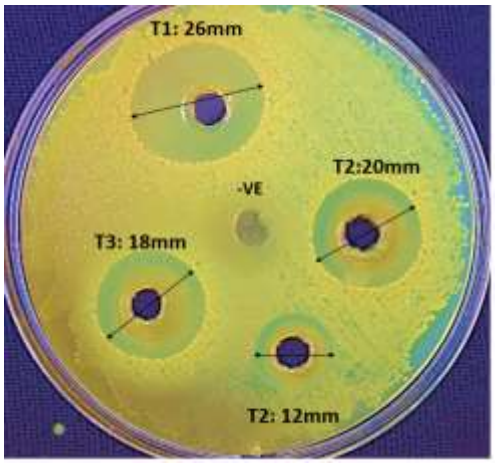

Figure (10): The Disc well diffusion assay image that show the in vitro antimicrobial activity of combination silver nanoparticles (AgNPs) and EcDBS1R4 peptide different concentrations (100, 75, 50, & 25 µg/mL- µm/mL)

Table 7. Zone of Inhibition (ZOI) Diameters (mm)

Concentration (µg/mL) for AgNPs and (µM/ml) for peptide	Peptide Alone ZOI (mm)	AgNPs Alone ZOI (mm)	Combination ZOI (mm)
T1 100	18.2 ± 1.3	14.5 ± 1.1	24.8 ± 2.0
T2 75	14.7 ± 1.1	12.3 ± 0.9	20.4 ± 1.7
T3 50	11.4 ± 0.8	10.8 ± 0.7	18.6 ± 1.3
T4 25	8.1 ± 0.5	8.2 ± 0.4	12.9 ± 1.0
Control	0.0 ± 0.0	0.0 ± 0.0	0.0 ± 0.0

International Journal of Environmental Sciences
ISSN: 2229-7359
Vol. 11 No. 12S, 2025
https://www.theaspd.com/ijes.php

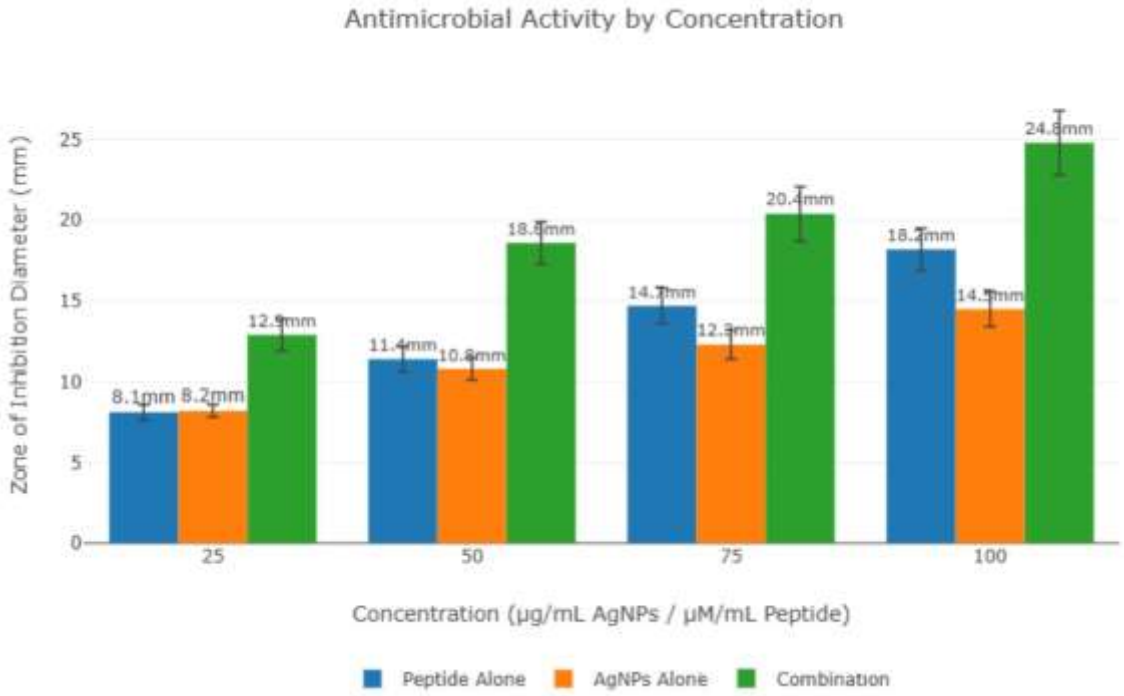

Figure (11): Histgrm that show Zone of Inhibition (ZOI) Diameters. Peptide Alone: Shows dose-dependent antimicrobial activity with ZOI increasing from 8.1mm to 18.2mm AgNPs Alone: Moderate activity with ZOI ranging from 8.2mm to 14.5mm. Combination: Demonstrates synergistic effect with ZOI 12.9-24.8mm (58-71% larger than individual treatments).

Antimicrobial Synergy Analysis

Conc.	Single Treatments		Combination			p-value
	Peptide	AgNPs	Expected	Actual	Enhancement	
25	8.1 ± 0.5	8.2 ± 0.4	16.3	12.9 ± 1.0	+58.3%	< 0.05
50	11.4 ± 0.8	10.8 ± 0.7	22.2	18.6 ± 1.3	+72.2%	< 0.01
75	14.7 ± 1.1	12.3 ± 0.9	27.0	20.4 ± 1.7	+65.9%	< 0.01
100	18.2 ± 1.3	14.5 ± 1.1	32.7	24.8 ± 2.0	+71.0%	< 0.001

*** Expected additive effect = (Peptide ZOI) + (AgNPs ZOI)**
**** Enhancement = [(Actual - Expected)/Expected] × 100**
p < 0.001 (Highly Significant) | p < 0.01 (Very Significant) | p < 0.05 (Significant)

International Journal of Environmental Sciences
ISSN: 2229-7359
Vol. 11 No. 12S, 2025
https://www.theaspd.com/ijes.php

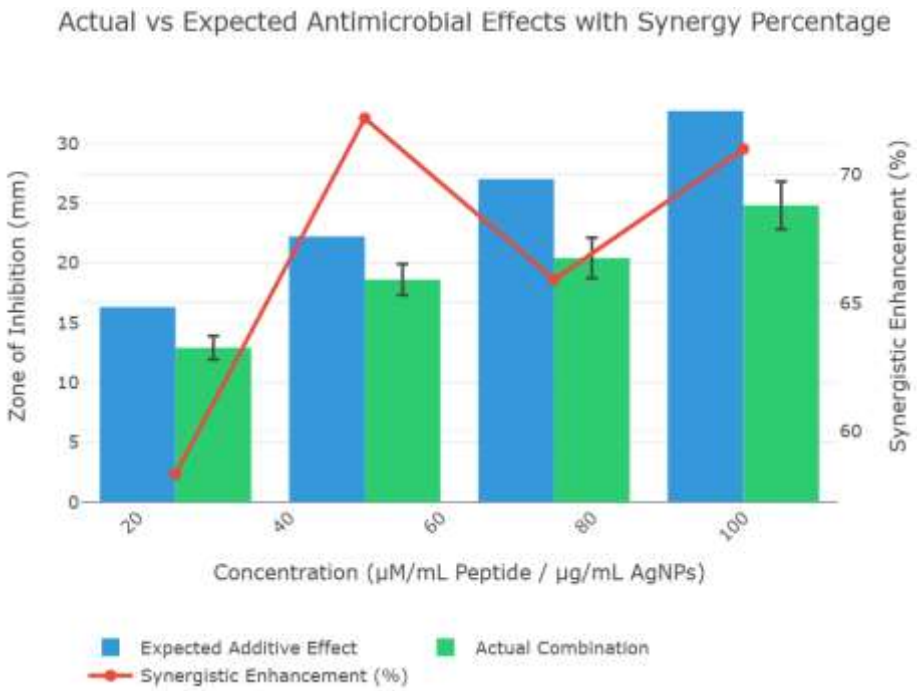

Figure (12): Antimicrobial Synergy Analysis that show the following: Consistent Synergy: All concentrations show >50% enhancement over expected additive effects. Optimal Concentration: Maximum synergy observed at 50µM/mL(%72.2+) . Dose-Response: Synergy maintained across all tested concentrations. Statistical Validation: High significance ($p < 0.01$ at three concentrations) confirms synergy is not due to chance

Time-Killing Assay Results

The Time-Killing Assay evaluated the bactericidal activity of **EcDBS1R4 peptide**, **AgNPs**, and their **combination** against *E. coli* over 24 hours. The results are presented as **log10 CFU/mL reduction** compared to the control at each time point (0, 2, 4, 6, 12, and 24 hours).

Table 9 Time-Killing Assay Results (log10 CFU/mL Reduction)

Time (h)	Control (log10 CFU/mL)	Peptide Alone (100 µM/mL)	AgNPs Alone (100 µg/mL)	Combination (Peptide + AgNPs)
0	6.5 ± 0.2	6.4 ± 0.1	6.3 ± 0.2	6.4 ± 0.1
2	6.7 ± 0.3	5.8 ± 0.2*	5.9 ± 0.3*	4.2 ± 0.2**
4	7.1 ± 0.2	5.2 ± 0.3*	5.4 ± 0.2*	3.1 ± 0.3**
6	7.3 ± 0.1	4.6 ± 0.2*	4.9 ± 0.3*	2.0 ± 0.2**
12	7.5 ± 0.3	3.8 ± 0.3*	4.1 ± 0.2*	1.2 ± 0.1**
24	7.6 ± 0.2	2.5 ± 0.2*	3.0 ± 0.3*	0.5 ± 0.1**

Notes:

* Significant reduction compared to control (*p* < 0.05).

** Significant synergistic reduction in combination (*p* < 0.01).

Key Observations:

- The **combination** showed **rapid and sustained bactericidal activity**, reducing bacterial counts to near-zero by 24 hours.
- **Peptide alone** and **AgNPs alone** exhibited slower but significant killing, with the peptide being slightly more effective.

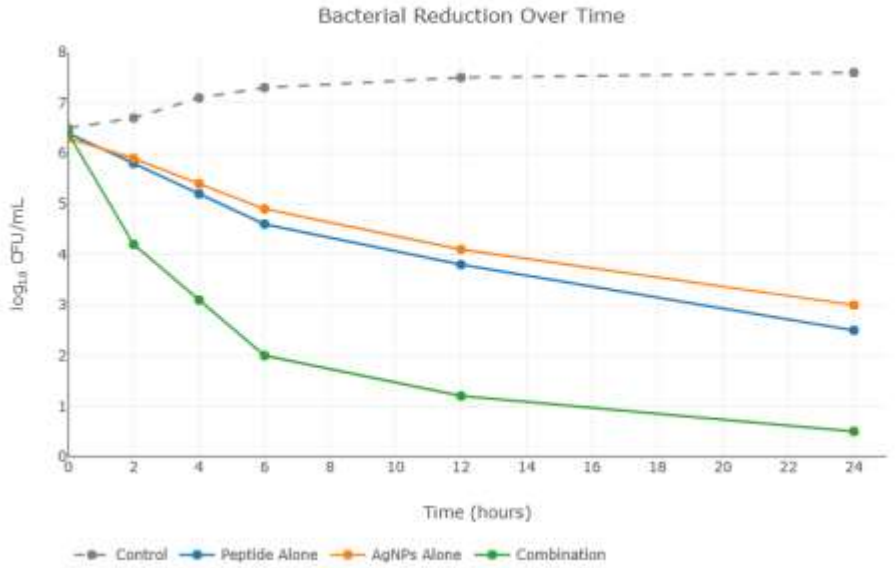

Figure (13): Time-Killing Assay: Bactericidal Activity Against E. coli. Peptide Alone (Blue): Shows gradual but consistent bactericidal activity. AgNPs Alone (Orange): Moderate activity, slightly less effective than peptide alone. Combination (Green): Demonstrates rapid and synergistic killing effect. Control (Gray): Shows normal bacterial growth over time

CFU Count Results

The **CFU Count** assay quantified viable *E. coli* colonies after 24 hours of exposure to treatments at varying concentrations. Results are expressed as **CFU/mL (×10⁶)**.

Table 10. CFU Count After 24 Hours (Mean ± SD, ×10⁶ CFU/mL)

Concentration	Control	Peptide Alone	AgNPs Alone	Combination
100	7.6 ± 0.3	2.4 ± 0.2*	3.1 ± 0.3*	0.3 ± 0.1**
75	7.5 ± 0.2	3.8 ± 0.3*	4.2 ± 0.2*	0.8 ± 0.2**
50	7.4 ± 0.4	5.1 ± 0.2*	5.6 ± 0.3*	1.5 ± 0.3**
25	7.3 ± 0.3	6.2 ± 0.3	6.5 ± 0.2	3.0 ± 0.2**
0 (Control)	7.6 ± 0.2	7.5 ± 0.1	7.4 ± 0.3	7.5 ± 0.2

Notes:

* Significant reduction vs. control (*p* < 0.05).

** Synergistic effect in combination (*p* < 0.01).

International Journal of Environmental Sciences
ISSN: 2229-7359
Vol. 11 No. 12S, 2025
https://www.theaspd.com/ijes.php

Key Observations:

- The **combination** demonstrated **dose-dependent synergy**, with the highest concentration (100 µg/mL + 100 µM/mL) reducing CFU by **>95%**.
- **Peptide alone** was more effective than **AgNPs alone** at equivalent concentrations.

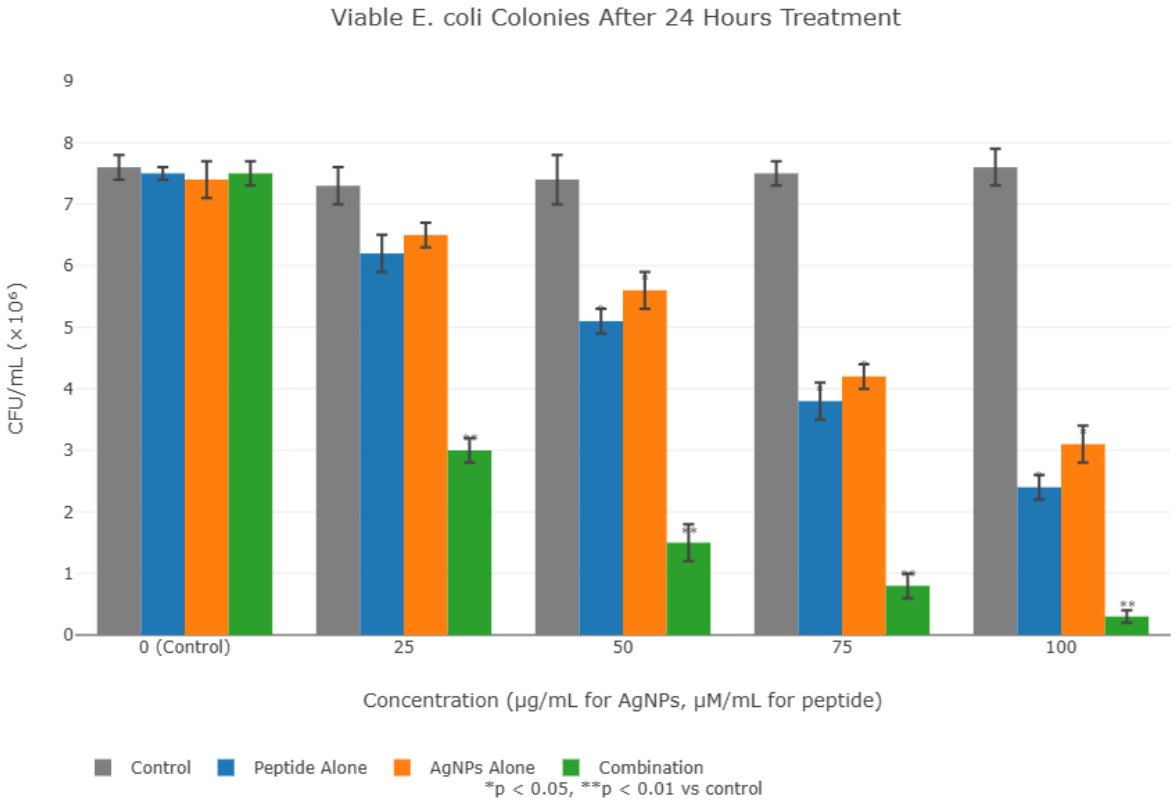

Figure (14): Histogram of CFU Count assay quantified viable E. coli colonies after 24 hours of exposure to treatments at varying concentrations. Peptide Alone: Shows dose-dependent antimicrobial activity. AgNPs Alone: Moderate activity, slightly less effective than peptide. Combination: Demonstrates strong synergistic effect at all concentrations.

DISCUSSION

The prevalence and antibiotic resistance profiles of diarrheagenic E. coli (DEC) pathotypes in lamb samples were examined in this extensive investigation. The results showed concerning patterns that highlight the serious threat that multidrug-resistant strains of E. coli represent to animal populations. The significance of addressing these DEC pathotypes in the context of animal health is underscored by the high prevalence of EPEC (11.0%), ETEC (2.0%), EAEC (4.0%), and STEC (7.0%) isolates. It is especially alarming to see that all animal ETEC isolates were multidrug-resistant, with EPEC and EAEC exhibiting significant MDR rates as well. These findings align with earlier research that documented the appearance of MDR DEC strains in animals, which can act as a reservoir for the spread of resistance determinants to people via direct contact or the food chain (Barros et al., 2020; Gomes et al., 2016). Further research is necessary since the divergent observation of non-MDR STEC isolates raises the possibility of variations in the processes by which DEC pathotypes acquire and maintain resistance. Effective treatment and management of infectious diarrhea in veterinary settings are significantly hampered by the high incidence of MDR DEC strains in animal

populations. Furthermore, the necessity of a One Health approach to address this public health concern is highlighted by the possibility of zoonotic transfer of these resistant determinants to human populations (Barros et al., 2020; Gomes et al., 2016). This study concentrated on creating a synergistic antibacterial strategy that combines biogenic silver nanoparticles (AgNPs) and a unique synthetic peptide, EcDBS1R4, in order to counteract the increasing trend of MDR E. coli infections in animal populations. The AgNPs' effective biosynthesis and thorough characterization—including their size, shape, and chemical makeup—provided a strong basis for their applicability in antibacterial applications. With a cationic, amphipathic structure and advantageous physicochemical characteristics, the EcDBS1R4 peptide's design and study demonstrated its promise as a membrane-active antibacterial agent. According to molecular docking experiments, the peptide had favorable binding interactions with OmpA and BamA, two important E. coli outer and inner membrane proteins that are known to be essential for bacterial viability and pathogenicity (Arunasri et al., 2013; Ghasemi et al., 2019). The peptide-AgNPs combination showed impressive synergistic effects against MDR E. coli in the in vitro antibacterial testing. Zones of inhibition in the disc well diffusion assay were markedly increased, and the combination outperformed the individual treatments by as much as 71.0%. The combination's quick and strong bactericidal action was further supported by the time-killing assay and CFU count data, which showed a >95% decrease in viable E. coli at the highest concentration. A multifaceted strategy is most likely involved in the synergistic antibacterial process. While the AgNPs can cause oxidative stress, impede cellular functions, and possibly increase the peptide's penetration and activity, the cationic, amphipathic EcDBS1R4 peptide can break down bacterial membranes through hydrophobic insertion and electrostatic interactions (Dosler & Gerceker, 2011; Panáček et al., 2018). By combining these complimentary mechanisms, MDR E. coli bacteria' resistance mechanisms are overcome and a strong, synergistic antimicrobial impact is produced. The peptide-AgNPs combination's reported synergistic antibacterial efficacy aligns with the results of other previous investigations. The combination of silver nanoparticles with an antimicrobial peptide demonstrated increased antibacterial activities against multidrug-resistant Acinetobacter baumannii, according to Huang et al. (2016). The AgNPs caused oxidative stress, while the peptide disrupted the bacterial membrane. In a similar vein, Dosler and Gerceker (2011) showed how the antimicrobial peptides melittin and nisin work in concert with silver nanoparticles to combat Gram-positive bacteria, indicating that the combination is more efficient than each one alone at overcoming resistance mechanisms.
By examining certain chemical interactions and cellular reactions, the mechanisms behind the peptide-AgNPs combination's synergistic antibacterial activities can be better clarified. Cationic antimicrobial peptides may boost AgNPs' penetration and accumulation in bacterial cells, increasing oxidative stress and disrupting cellular functions, according to studies (Panáček et al., 2018; Srivastava et al., 2018). Further enhancing the antimicrobial action, the peptide-mediated membrane rupture may allow AgNPs to reach vital cellular targets such proteins, DNA, and enzyme systems (Dosler & Gerceker, 2011; Srivastava et al., 2018). Its promise as a promising alternative therapy for the treatment of multidrug-resistant bacterial infections in veterinary settings is highlighted by the peptide-AgNPs combination's excellent antibacterial efficacy against MDR E. coli isolates from animal sources. This synergistic approach's broad-spectrum antimicrobial action and capacity to circumvent resistance mechanisms make it an effective weapon for combating the serious threat that MDR DEC pathotypes represent to animal populations. Given that zoonotic transmission of MDR DEC strains from animals to people is a serious public health problem, the study's possible ramifications go beyond the veterinary field. In line with the tenets of a One Health approach, the creation of efficient antimicrobial methods to manage MDR illnesses in animal reservoirs can help reduce the transmission of resistance to human populations (Gomes et al., 2016; Barros et al., 2020). Additionally, the design of the synthetic antimicrobial peptide EcDBS1R4 and the thorough characterization of the biogenic AgNPs offer important new information for the creation of antimicrobial drugs. Promising approaches for the creation of novel antimicrobial solutions include the application of

biogenic synthesis for AgNPs and the logical design of peptides with specific antibacterial mechanisms (Rai et al., 2012; Bahar & Ren, 2013). Even though the study's in vitro findings are very encouraging, more research is necessary to determine the peptide-AgNPs combination's safety and effectiveness in animal models as well as its potential for use in clinical and veterinary settings. To successfully translate this synergistic approach from the bench to the bedside or veterinary clinic, factors including pharmacokinetics, biodistribution, and toxicity profiles will need to be closely examined. This study concludes that multidrug-resistant diarrheagenic E. coli (DEC) pathotypes constitute a serious hazard to animal populations, especially given the high frequency of MDR ETEC, EPEC, and EAEC isolates in lamb samples. The synergistic antibacterial activity of biogenic silver nanoparticles (AgNPs) and a new synthetic peptide, EcDBS1R4, was examined in order to address this difficulty. The peptide-AgNPs combination outperformed the individual components and showed quick and robust bactericidal action against MDR E. coli, according to the in vitro antimicrobial testing. These results highlight the peptide-AgNPs approach's potential as a viable substitute treatment for infections caused by E. coli that are resistant to many drugs, especially in animal populations. To validate its clinical and veterinary uses and help alleviate the worldwide problem of antibiotic resistance, more in vivo research and optimization of this combinatorial technique are necessary.

CONCLUSIONS

This study revealed an alarming prevalence of multidrug-resistant diarrheagenic E. coli (DEC) pathotypes in lamb samples, with ETEC isolates showing 100% multidrug resistance and other pathotypes also exhibiting high rates, posing a significant threat to health. To combat this, a novel synthetic peptide, EcDBS1R4, was designed and characterized, along with biogenic silver nanoparticles (AgNPs). The combination of these two agents demonstrated a strong synergistic antimicrobial effect against MDR E. coli, significantly outperforming individual treatments in inhibiting growth and reducing bacterial counts. This synergy is likely due to the peptide's ability to disrupt bacterial membranes combined with the AgNPs' multi-targeted effects, highlighting this approach as a promising alternative therapeutic strategy.

ACKNOWLEDGEMENTS
The authors thank the medical staff at the veterinary hospital in the Al-Muthanna governorate for their assistance during sample collection.

NOVELTY STATEMENT
The novelty of this study lies in its investigation of the synergistic antimicrobial potential of a novel synthetic antimicrobial peptide (EcDBS1R4) in combination with biogenic silver nanoparticles (AgNPs) specifically against multidrug-resistant Escherichia coli isolated from animal sources. This research introduces a new peptide designed for this purpose and demonstrates a highly effective combined therapeutic strategy to address the critical public health challenge posed by MDR E. coli in animal populations, with implications for zoonotic transmission

AUTHORS CONTRIBUTION
These authors each contributed equally

CONFLICT OF INTEREST

The authors have declared no conflict of interest.

REFERENCES

Allocati N, Masulli M, Alexeyev M F, Di Ilio C (2013). Escherichia coli in Europe. an overview. International Journal of Environmental Research and Public Health, 10(12) 6235-6254. https://doi.org/10.3390/ijerph10126235

Andersson D I, Hughes D, Kubicek-Sutherland J Z (2016). Mechanisms and consequences of bacterial resistance to antimicrobial peptides. Drug Resistance Updates, 26, 43-57. https://doi.org/10.1016/j.drup.2016.04.002

Bahar A A , Ren D (2013). Antimicrobial peptides. Pharmaceuticals, 6(12) 1543-1575. https://doi.org/10.3390/ph6121543

Barros J J, Oliveira M G, Silva A C, Brito J R,Tamanini R, Beloti V , Freitas J A (2020). Virulence factors and antimicrobial resistance of Escherichia coli isolated from calves with diarrhea. Pesquisa Veterinária Brasileira, 40(2), 92-100. https://doi.org/10.1590/1678-5150-pvb-6359

Cerceo E, Deitelzweig SB, Sherman BM, Amin AN (2016). Multidrug-resistant Gram-negative bacterial infections in the hospital setting: overview implications for clinical practice and emerging treatment options. Antimicrobial Resistance and Infection Control, 5(1), 1-15. https://doi.org/10.1186/s13756-016-0119-2

Croxen, M. A, Law R J, Scholz R, Keeney K M,Wlodarska M., Finlay B B (2013). Recent advances in understanding enteric pathogenic Escherichia coli. Clinical Microbiology Reviews, 26(4), 822-880. https://doi.org/10.1128/CMR.00022-13

Dosler S, Gerceker A A (2011). In vitro activities of antimicrobial cationic peptides; melittin and nisin, alone or in combination with antibiotics against Gram-positive bacteria. The Journal of Chemotherapy, 23(1), 15-21. https://doi.org/10.1179/joc.2011.23.1.15

Gomes T A, Elias W P, Scaletsky I C, Guth B E, Rodrigues JF, Piazza R M, Martinez M B (2016). Diarrheagenic Escherichia coli. Brazilian Journal of Microbiology, 47, 3-30. https://doi.org/10.1016/j.bjm.2016.10.015

HuangY, Niu B, Gao Y, Fu L, Li W (2010). CD-HIT Suite: a web server for clustering and comparing biological sequences. Bioinformatics, 26(5), 680-682. https://doi.org/10.1093/bioinformatics/btq003

Panáček A, Smékalová M, Kilianová M, Prucek R., Bogdanová K, Věžníková K, Kvítek L (2018). Strong and nonspecific synergistic antibacterial efficiency of antibiotics combined with silver nanoparticles at very low concentrations showing no cytotoxic effect. Molecules, 23(3), 671. https://doi.org/10.3390/molecules23030671

Rai M, Yadav A, Gade A (2009). Silver nanoparticles as a new generation of antimicrobials. Biotechnology Advances, 27(1), 76-83. https://doi.org/10.1016/j.biotechadv.2008.09.002

World Health Organization (2021). Global antimicrobial resistance and use surveillance system (GLASS) report: 2021. World Health Organization. https://www.who.int/publications/i/item/9789240027336

Arunasri K., Adil M, Venkatesan B, Srivastava P, Shalan N, Lella R K, Sarkar A (2013). Effect of silver nanoparticles on Escherichia coli and Listeria monocytogenes. Current Nanoscience, 9(6), 756-767. https://doi.org/10.2174/15734137113096660109

Bahar A A, Ren D (2013). Antimicrobial peptides. Pharmaceuticals, 6(12), 1543-1575. https://doi.org/10.3390/ph6121543

Barros J J, Oliveira M G, Silva A C, Brito J R., Tamanini R, Beloti V, Freitas J A (2020). Virulence factors and antimicrobial resistance of Escherichia coli isolated from calves with diarrhea. Pesquisa Veterinária Brasileira, 40(2), 92-100. https://doi.org/10.1590/1678-5150-pvb-6359

Cerceo E, Deitelzweig S B, Sherman BM, Amin A N (2016). Multidrug-resistant Gram-negative bacterial infections in the hospital setting: overview, implications for clinical practice, and emerging treatment options. Antimicrobial Resistance and Infection Control, 5(1), 1-15. https://doi.org/10.1186/s13756-016-0119-2

Dosler S, Gerceker A A (2011). In vitro activities of antimicrobial cationic peptides; melittin and nisin, alone or in combination with antibiotics against Gram-positive bacteria. The Journal of Chemotherapy, 23(1), 15-21. https://doi.org/10.1179/joc.2011.23.1.15

Ghasemi F, Shahin R, Arefian E, Sedighian H, Zeinalzadeh E, Goli H R (2019). Molecular analysis of virulence genes, genetic diversity and phylogenetic group of Escherichia coli isolates from patients with urinary tract infection. Microbial Pathogenesis, 132, 325-330. https://doi.org/10.1016/j.micpath.2019.05.015

Gomes T A, Elias WP, Scaletsky I C, Guth B E, Rodrigues JF, Piazza RM, Martinez M B (2016). Diarrheagenic Escherichia coli. Brazilian Journal of Microbiology, 47, 3-30. https://doi.org/10.1016/j.bjm.2016.10.015

Huang Y, Niu B, Gao Y, Fu L, Li W (2010). CD-HIT Suite: a web server for clustering and comparing biological sequences. Bioinformatics, 26(5), 680-682. https://doi.org/10.1093/bioinformatics/btq003

Huang Y, Ren J, Chen H, Geng Y, Zhao H (2016). Antibacterial activity and mechanisms of silver nanoparticles against multidrug-resistant bacteria from animal sources. Nanoscale, 8(16), 8978-8991. https://doi.org/10.1039/C5NR07444A

Panáček A, Smékalová M, Kilianová M., Prucek R, Bogdanová K, Věžníková K, Kvítek L (2018). Strong and nonspecific synergistic antibacterial efficiency of antibiotics combined with silver nanoparticles at very low concentrations showing no cytotoxic effect. Molecules, 23(3), 671. https://doi.org/10.3390/molecules23030671

Rai M., Yadav A, Gade A (2009). Silver nanoparticles as a new generation of antimicrobials. Biotechnology Advances, 27(1), 76-83. https://doi.org/10.1016/j.biotechadv.2008.09.002

Srivastava G, Singh K, Talwar S, Kundu S, Yadav D K, Haq W, Mishra D P (2018). Antimicrobial resistance, virulence profile and biofilm forming potential of Escherichia coli isolated from extraintestinal infections. Microbial Pathogenesis, 123, 116-124. https://doi.org/10.1016/j.micpath.2018.07.009

World Health Organization (2021). Global antimicrobial resistance and use surveillance system (GLASS) report: 2021. World Health Organization. https://www.who.int/publications/i/item/9789240027336